Measurement Structures and Constraints in Compressive RF Systems

Nathan A. Goodman
School of Electrical and Computer Engineering
Advanced Radar Research Center
The University of Oklahoma, Norman, Oklahoma 73019
goodman@ou.edu

***Abstract*—Compressive sensing (CS) is a powerful technique for sub-sampling of signals combined with reconstruction based on sparsity. Many papers have been published on the topic; however, they often fail to consider practical hardware factors that may prevent or alter the implementation of desired CS measurement kernels. In particular, different compressive architectures in the RF domain either sacrifice collected signal energy or create noise folding, both of which cause SNR reduction. In this paper, we consider valid signal models and other system aspects of RF compressive systems.**

I. Introduction

Interest in the application of compressive sensing (CS) to radar and other radio frequency (RF) applications has grown rapidly. This interest is fueled by the potential to implement RF systems that perform well while reducing the burden on data collection hardware. For example, the idea of a sparsely populated or thinned array has been used for a long time as a way of obtaining high resolution from a long array baseline without the cost and weight of a fully populated array. The difference in recent years is that CS principles are now being used to design the array, to analyze its performance, and to process its data via sparse reconstruction methods. Similar statements can be made regarding other examples of compressive RF systems (not just antenna arrays).

The current literature on compressive RF systems is skewed toward demonstrating the ability to recover signals from such systems using sparse reconstruction methods. While this approach is interesting, there is still a shortage of analysis on the system impacts of RF compression and on the ultimate performance of compressive RF systems in useful exploitation tasks such as signal detection and parameter estimation. Unfortunately, some published papers also fail to consider the architecture of the compressive system and resulting constraints that this architecture imposes on the structure of the compression kernels and the relevant signal model.

In this paper, we address some of these structural and system considerations in compressive RF systems. We consider fundamental models of measurement as linear projections implemented in time and space, and map these models to appropriately structured sensing matrices for several types of compressive RF sensing. We then focus on compression via sub-Nyquist analog-to-digital conversion (ADC) and consider a compressive version of the traditional quadrature receiver.

II. Models for RF Compression

In this section, we start with a model for conventional sampling and map that model to the matrix-vector notation typically used in CS. We then use the model to represent two types of compression that RF systems might employ, namely measurement "thinning" and measurement "mixing". We also discuss the inclusion of additive receiver noise in the models.

Let a compressive RF receiver observe a signal, $s(\mathbf{r},t)$, that varies over space and time where $\mathbf{r}$ is a three-dimensional vector of spatial coordinates. Let the compressive system comprise a P-element antenna array with element coordinates $\mathbf{r}_p$ and each element having its own receiver. We can express a "traditional" sample as the projection of the signal onto a measurement kernel that is localized in time and space. In ideal sampling, this kernel is an impulse-like space-time function located at the element position and sample time where the sample is to occur, such that

$$\begin{aligned} s(\mathbf{r}_p,t_n) &= \left\langle s(\mathbf{r},t), \delta(\mathbf{r}-\mathbf{r}_p)\delta(t-t_n)\right\rangle \\ &= \iint s(\mathbf{r},t)\delta(\mathbf{r}-\mathbf{r}_p)\delta(t-t_n)\,d\mathbf{r}dt \end{aligned} . \quad (1)$$

We can then express data collected by the array and sampled over time by a set of impulsive measurement kernels located at every element location and sampling time instant.

In order to represent (1) with a discrete model suitable for computer simulations or manipulation via linear algebra, we can approximate the integral in (1) with a summation over small, finite-sized *bins* in space and time, such that

$$\begin{aligned} &\iint s(\mathbf{r},t)\delta(\mathbf{r}-\mathbf{r}_p)\delta(t-t_n)\,d\mathbf{r}dt \approx \\ &\qquad \Delta\mathbf{r}\Delta t\sum_{\mathbf{r}(i)}\sum_{t(j)} s(\mathbf{r}(i),t(j))\delta\left[\mathbf{r}(i)-\mathbf{r}_p\right]\delta\left[t(j)-t_n\right] \end{aligned} \quad (2)$$

where $\mathbf{r}(i)$ denotes the ith spatial bin in the approximation, $t(j)$ denotes the jth temporal bin, and the delta function with brackets, $\delta[\cdot]$ is used to denote the Kronecker delta function that is equal to one when the argument is zero (to within the quantization error of the bins) and zero elsewhere. If the bins are chosen smaller than or equal to the Nyquist sampling interval, then the discrete approximation will be accurate.

Next, we form a signal vector by taking all signal values over the discrete bins and organizing them into a vector according to a specific ordering; for example,

$$\mathbf{s} = \begin{bmatrix} s(\mathbf{r}(1), t(1)) \\ s(\mathbf{r}(1), t(2)) \\ s(\mathbf{r}(1), t(3)) \\ \vdots \\ s(\mathbf{r}(N_s), t(N_t)) \end{bmatrix} \tag{3}$$

where N_s is the number of discrete bins covering the signal's spatial volume and N_t is the number of discrete bins covering the signal's temporal duration. The length of $\mathbf{s}$ is $N = N_t N_s$. The expression in (2) can then be expressed as

$$\begin{aligned} &\iint s(\mathbf{r},t)\delta(\mathbf{r}-\mathbf{r}_p)\delta(t-t_n)\,d\mathbf{r}dt \\ &\quad \approx \Delta\mathbf{r}\Delta t\begin{bmatrix}0 & \cdots & 0 & 1 & 0 & 0 & \cdots & 0\end{bmatrix}\mathbf{s} \\ &\quad = \Delta\mathbf{r}\Delta t\boldsymbol{\delta}_m\mathbf{s} \end{aligned} \tag{4}$$

where $\boldsymbol{\delta}_m$ is defined (as shown) as a row vector with zeros everywhere except in the entry corresponding to the discretized bin where the mth data sample is collected. A sampling matrix can then be represented as a collection of $\boldsymbol{\delta}_m$'s, with each row having the '1' in a different location. For example, if only three data samples are collected, the sensing matrix might look like

$$\boldsymbol{\Phi} = \begin{bmatrix}\boldsymbol{\delta}_1 \\ \boldsymbol{\delta}_2 \\ \boldsymbol{\delta}_3\end{bmatrix} = \begin{bmatrix}1 & 0 & 0 & 0 & \cdots & 0 \\ 0 & 0 & 1 & 0 & \cdots & 0 \\ 0 & 0 & 0 & 0 & \cdots & 1\end{bmatrix}. \tag{5}$$

The matrix in (5) represents a "thinning" type of compression where the sampling kernels are still localized in space and time, but not all signal elements are sampled. Some radar-specific examples of where this type of compression might occur include 1) some pulses in a coherent pulse train are not transmitted, causing gaps in the slow-time data collection, 2) the thinned or sparse antenna array mentioned above, and 3) stepped-frequency waveforms where frequency steps can be skipped in the data collection process [1]. In these structures, there will be groups of nearby samples taken at the Nyquist rate, followed by gaps in the sampling. Full Nyquist sampling can also be represented by using $\boldsymbol{\Phi} = \mathbf{I}_N$.

On the other hand, the "thinning" type compression depicted in (5) is usually not a suitable representation for compression in the ADC process (i.e., in fast time). For the examples above, it is easy to envision how some samples will be closely spaced (for example, two pulses in a row), but

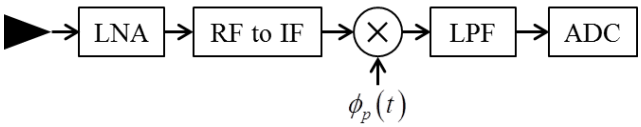

Figure 1. Block diagram of sub-Nyquist, fast-time compression implemented at an intermediate frequency (IF).

for fast-time compression, the thinning approach means that the ADC must occasionally collect samples at the full bandwidth of the signal. If the ADC must have the capability to sample at the full bandwidth, then the hardware advantages of compressive sampling disappear. Therefore, fast-time compression will typically be implemented with an ADC operating at a uniform sampling rate lower than the Nyquist rate. In order to avoid aliasing, the signal must be mixed with a non-localized measurement kernel before being sampled; therefore, this second form of compression is a "mixing" type compression that requires an analog multiplication. Hardware structures for sub-Nyquist sampling, including the random demodulator [2] and the modulated wideband converter [3] fall into this category of compression. A block diagram of an example RF compressive receiver is shown in Figure 1 where we can see the required elements including low-noise amplifier (LNA), downconversion from RF frequency to an intermediate frequency (IF) where analog multiplication with another wideband kernel can be performed, a lowpass filter to complete the projection, and finally sampling at a sub-Nyquist rate.

Mixing type compression can be represented in the projection notation above by replacing the localized delta sampling functions with an arbitrary measurement kernel according to

$$\begin{aligned} &\iint s(\mathbf{r},t)\phi(\mathbf{r},t)\,d\mathbf{r}dt \approx \\ &\qquad \Delta\mathbf{r}\Delta t\sum_{\mathbf{r}(i)}\sum_{t(j)} s(\mathbf{r}(i),t(j))\phi(\mathbf{r}(i),t(j)). \end{aligned} \tag{6}$$

If the compression is being performed via sub-Nyquist sampling of the signal captured by a particular antenna element, then the spatial component of the measurement kernel can be localized such that

$$\begin{aligned} &\iint s(\mathbf{r},t)\delta(\mathbf{r}-\mathbf{r}_p)\phi_p(t)\,d\mathbf{r}dt \approx \\ &\qquad \Delta\mathbf{r}\Delta t\sum_{\mathbf{r}(i)}\sum_{t(j)} s(\mathbf{r}(i),t(j))\delta[\mathbf{r}(i)-\mathbf{r}_p]\phi_p(t(j)) \end{aligned} \tag{7}$$

where $\phi_p(t)$ is the temporal mixing kernel applied to the receiving chain of the pth antenna element. For sub-Nyquist sampling on multiple antenna elements, the sensing matrix representation will be a composite of the thinning structure (due to elements that may or may not be present) with a structure that implements the non-localized temporal kernels.

Until a technology exists to implement the temporal modulation component of the measurement kernel directly at the antenna (using, for example, current distributions on an antenna element varying at the bandwidth of the incoming signal), the fast-time compression must be implemented with hardware such as analog multipliers, mixers, and filters as

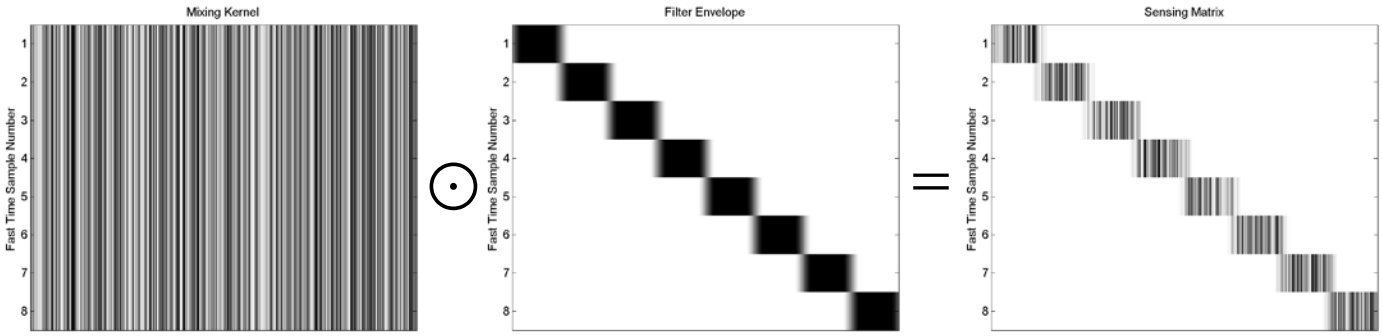

Figure 2. Structure of a sensing matrix for fast-time compression using analog multiplication followed by lowpass filtering.

depicted in Figure 1. There are two implications of the architecture in Figure 1. First, because the compression is performed after the signal has entered the receiver, additive receiver noise must be applied to the signal prior to the compression operation, which leads to noise folding [4], or more generally a loss in signal-to-noise ratio (SNR). Second, the time duration over which the signal is integrated (and, therefore, the length of any single projection) is determined by the time support of the lowpass filter's impulse response. Each successive sample taken by the ADC will be the result of integrating approximately T_c seconds of multiplier output where T_c is the approximate duration of the filter's impulse response. If the ADC sampling interval, T_{ADC}, is less than T_c, then successive samples will be partially correlated due to overlapping integration periods. Typically, we will set $T_{ADC} = T_c$ such that each sample is a result of an adjacent, and approximately non-overlapping, integration period.

Considering the above statements, (7) can be modified as

$$\begin{aligned}&\int\left[\left(s(\mathbf{r},t)\delta(\mathbf{r}-\mathbf{r}_p)\phi_p(t)+n_p(t)\right)*h(t)\right]d\mathbf{r}\\&=\int\left(s(\mathbf{r}_p,\tau)\phi_p(\tau)+n_p(\tau)\right)h(t-\tau)\,d\tau\\&\approx\Delta t\sum_{\tau(j)}\left(s(\mathbf{r}_p,\tau(j))\phi_p(\tau(j))+n_p(\tau(j))\right)h(t-\tau(j))\end{aligned}\quad,\quad(8)$$

which introduces a precise structure to the sensing matrix for each antenna element. This structure, which is depicted in Figure 2 (right panel) for compression down to eight ADC samples on a single antenna element, is a combination of the mixing kernel (left panel) and the LPF's impulse response shifted to implement the correct convolution output at the ADC sample times (middle panel). The discrete sensing model is then

$$\mathbf{y}_p=\mathbf{\Phi}_p\left(\mathbf{s}_p+\mathbf{n}_p\right)\quad(9)$$

where $\mathbf{s}_p$ is the temporally varying signal incident on the pth antenna, $\mathbf{n}_p$ is the additive noise on the pth receiving channel, and $\mathbf{\Phi}_p$ is the fast-time sensing matrix for the pth channel in the structure shown in Figure 2 according to the ADC rate, filter impulse response, and pth channel's mixing kernel $\phi_p(t)$. An overall space-time sensing matrix can then be expressed by concatenating the sensing matrices for individual channels according to a pattern along the lines of

$$\mathbf{\Phi}=\begin{bmatrix}\mathbf{\Phi}_1&\mathbf{0}&\mathbf{0}&\mathbf{0}&\mathbf{0}&\cdots&\mathbf{0}\\\mathbf{0}&\mathbf{0}&\mathbf{\Phi}_2&\mathbf{0}&\mathbf{0}&&\mathbf{0}\\\mathbf{0}&\mathbf{0}&\mathbf{0}&\mathbf{\Phi}_3&\mathbf{0}&&\mathbf{0}\\\mathbf{0}&\mathbf{0}&\mathbf{0}&\mathbf{0}&\mathbf{0}&&\mathbf{0}\\\mathbf{0}&\mathbf{0}&\mathbf{0}&\mathbf{0}&\mathbf{0}&\ddots&\vdots\\\mathbf{0}&\mathbf{0}&\mathbf{0}&\mathbf{0}&\mathbf{0}&\ddots&\mathbf{0}\\\mathbf{0}&\mathbf{0}&\mathbf{0}&\mathbf{0}&\mathbf{0}&\cdots&\mathbf{\Phi}_P\end{bmatrix}\quad(10)$$

where blocks of columns containing all zeros are due to missing antenna elements that have been thinned from the system. The resulting measurements are

$$\mathbf{y}=\mathbf{\Phi}\left(\mathbf{s}+\mathbf{n}\right)\quad(11)$$

where $\mathbf{s}$ and $\mathbf{n}$ have been formed by concatenating the signal and noise vectors for all antenna elements, including elements not sampled by the sensing matrix.

The model in (11) shows noise added prior to application of the sensing matrix (pre-projection noise model) for many reasons. First, even though the zero columns of the sensing matrix may result in a larger representation than necessary, the full representation reinforces the true input dimensionality of the space-time, Nyquist-sampled signal. Second, as described earlier, pre-projection noise is the correct representation for mixing-type compression implemented in analog hardware. Third, while faithfully representing mixing-type compression, the full representation also encompasses thinning-type compression as a special case. The sensing model in (11) can be expressed as

$$\mathbf{y}=\mathbf{\Phi s}+\mathbf{\Phi n}=\mathbf{\Phi s}+\hat{\mathbf{n}}\quad(12)$$

where the post-projection noise covariance matrix can be easily calculated from the pre-projection covariance and the sensing matrix. Therefore, the post-projection additive noise model used in some of the RF CS literature is valid in certain situations, but (12) explicitly shows that care must be taken in considering the post-projection noise statistics. If the input noise is uncorrelated and the rows of $\mathbf{\Phi}$ are orthogonal, then it is valid to go directly to a post-projection uncorrelated additive noise model, but in general, post-projection noise skips over a more fundamental starting point that may be helpful for proper treatment of system constraints and noise statistics. Finally, the full representation admits interpretation

of SNR loss due to compression as a loss in collected signal energy, as a noise folding behavior, or both. From the zero columns in (10), it is easy to see that for every measurement that is removed, collected signal energy is lowered. Radar systems are typically limited in transmit power and can't arbitrarily transmit additional power to make up for fewer samples. It is easy to ignore this loss or model it improperly when starting from a post-projection additive noise model.

III. Quadrature Compression

Many RF receivers implement quadrature reception where the down-conversion from RF (or IF) to baseband results in an in-phase (I) branch and a quadrature (Q) branch. These branches are 90 degrees out of phase with respect to each other such that signals with a random phase component are captured by one of the branches or a combination of the two. In this section we consider I/Q compression and its impact on the relationship between the I and Q signals.

A narrowband bandpass signal can be represented as

$$s(t) = a(t)\cos\left(2\pi F_0 t + \theta(t) + \theta_0\right) \tag{13}$$

where $a(t)$ and $\theta(t)$ are amplitude and phase modulations, respectively, with modulation bandwidths, B, much smaller than the carrier frequency F_0. The signal is assumed to have an unknown global phase θ_0. Without knowledge of θ_0, if we demodulate with only the cosine of the carrier, we risk demodulating with a carrier term that is out of phase with the received carrier, and the signal will be lost. Therefore, quadrature receivers demodulate against quadrature components of the carrier, guaranteeing signal capture regardless of global phase. However, because the receiver has I and Q branches, compression should be performed in each.

Figure 3 shows a potential architecture for a compressive quadrature receiver (hardware considerations may mean that the best design is a two-stage downconversion, but the format in Figure 3 is sufficient for the sampling analysis considered here). The incoming signal is split into two branches. The in-phase branch is demodulated with a cosine of the carrier and the quadrature branch is demodulated with a sine of the carrier. The first LPF in each branch has cutoff frequency at or above $B/2$ where B is the signal's bandpass bandwidth and is meant to reject all but the baseband copy of the signal. Next, the signal is mixed with a compression kernel, which might be a different kernel for the I and Q brances, followed by a LPF that completes the projection. The second LPF's in each branch have the same cutoff frequency, which is related to the sub-Nyquist sampling rate.

After passing the signal in (13) through the first mixer/LPF pair (downconversion step), the resulting signals are

$$\tilde{s}_I(t) = \frac{1}{2}a(t)\cos\left(\theta(t) + \theta_0\right) \tag{14}$$

and

$$\tilde{s}_Q(t) = \frac{1}{2}a(t)\sin\left(\theta(t) + \theta_0\right) \tag{15}$$

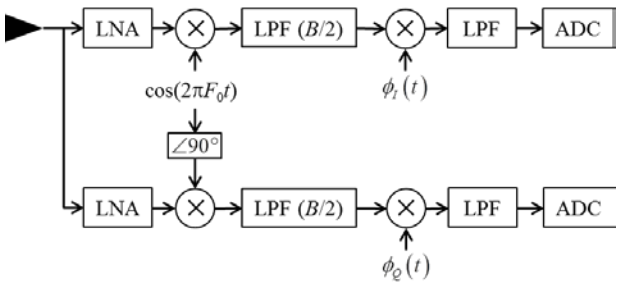

Figure 3. Compressive I/Q receiver architecture.

in the I and Q branches, respectively. These signals are then separately compressed by passing them through the second multiplier/LPF pair corresponding to the compression kernels in each branch, $\phi_I(t)$ and $\phi_Q(t)$. Letting the matrix-vector representations of (14) and (15) be $\tilde{\mathbf{s}}_I$ and $\tilde{\mathbf{s}}_Q$, respectively, the compressed data samples for the two branches are

$$\mathbf{y}_I = \mathbf{\Phi}_I\left(\tilde{\mathbf{s}}_I + \tilde{\mathbf{n}}_I\right) \tag{16}$$

and

$$\mathbf{y}_Q = \mathbf{\Phi}_Q\left(\tilde{\mathbf{s}}_Q + \tilde{\mathbf{n}}_Q\right). \tag{17}$$

In the absence of compression, the outputs of the two branches are typically treated as orthogonal and placed as the real and imaginary components of complex-valued data samples. Compression, however, decreases the distance between the two components. Therefore, the fundamental I/Q relationship may be altered, which may impact traditional processing steps such as envelope detection. Appropriate detectors and estimators for compressive quadrature receivers have yet to be fully developed in the literature.

IV. Conclusions

We have consider several aspects of compressive RF sensing, including appropriate signal and noise models for compression in different dimensions (slow time, fast time, spatial) and corresponding constraints on sensing matrices. We have also begun to consider a compressive version of the traditional quadrature receiver and the impacts that compression of in-phase and quadrature components may have on subsequent processing algorithms.

Acknowledgment

We acknowledge support from the Defense Advanced Research Projects Agency via grant #N66001-10-1-4079.

References

[1] L. Anitori, et al., "Design and analysis of compressed sensing radar detectors," *IEEE Trans. Sig. Proc.*, vol. 61, no. 4, pp. 813-827, Feb. 2013.

[2] J.A. Tropp, et al., "Beyond Nyquist: efficient sampling of sparse bandlimited signals," *IEEE Trans. Info.Theory*, vol. 56, no. 1, pp. 520-544 (2010).

[3] M. Mishali and Y.C. Eldar, "From theory to practice: sub-Nyquist sampling of sparse wideband analog signals," *IEEE J. Sel. Topics Sig. Proc.*, vol. 4, no. 2, pp. 375 – 391 (2010).

[4] E. Arias-Castro and Y. Eldar, "Noise folding in compressed sensing," *IEEE Sig. Proc. Letters*, vol. 18, no. 8, pp. 478-481 (2011).